Revista Mexicana de Física S **58** (2) 245–248 DICIEMBRE 2012

Hall magnetometry in a closed-cycle refrigerator

J. Fernandez Pinto, F.L.A. Machado, and A.R. Rodrigues
Departamento de Física, Universidade Federal de Pernambuco, Recife, 50670-901, Pernambuco, Brazil.
e-mail: flam@df.ufpe.br

Recibido el 25 de junio de 2010; aceptado el 9 de mayo de 2011

A small size and not expensive Hall magnetometer was built using two Toshiba GaAs (THS118) Hall sensors operating in a differential mode. The Hall magnetometer was assembled in a closed-cycle refrigerator for data acquisition from room temperature down to 10 K. The system was used to study the effect of the cooling magnetic field (H_R) in the exchange-bias field (H_{EB}) in the nanocomposite $(Fe_{0.6}Co_{0.4})_{0.35}(MnO)_{0.65}$ at low temperatures. It was found that the H_{EB} first increases for increasing values of H_C, it reaches a maximum value (=22.5 mT) for H_R = 0.5 T and it diminishes when H_R is further increased, yielding 17 mT for H_R = 1 T.

Keywords: Hall magnetometer; exchange-bias effect; nanocomposite.

Un magnetómetro Hall de tamaño pequeño y bajo costo fue construido utilizando dos sensores Hall, Toshiba GaAs (THS118), operando en modo diferencial. Este magnetómetro fue adaptado a un criostato de ciclo cerrado en el que se pueden adquirir datos desde temperatura ambiente hasta 10 K. Este equipo de medición fue utilizado para estudiar el efecto del campo magnético de enfriamiento (H_R) sobre el campo magnético de intercambio (H_{EB}) en el nanocomposito $(Fe_{0.6}Co_{0.4})_{0.35}(MnO)_{0.65}$, a temperaturas bajas. Encontramos que H_{EB} primero aumenta para valores crecientes de H_C, alcanzando un valor máximo de 22.5 mT para H_R= 0.5 T y luego disminuye cuando H_R continua aumentando alcanzando un valor de 17 mT para H_R= 1T.

Descriptores: Magnetómetro Hall, efecto exchange-bias; nanocompuestos.

PACS: 75.50.Tt; 75.60.Ej; 75.30.-m

1. Introduction

Hall effect based magnetometers has been used to investigate magnetic materials for many years already [1-3]. Among the characteristics that make these magnetometers attractive are the low cost, they can easily be constructed and their operation is relatively simple. The Hall magnetometer has no moving parts in contrast with other techniques. It does not require, for instance, the sample be moved through magnetic coils like in the extraction and in the vibrating sample magnetometers. Thus, the Hall magnetometers can easily be assembled in a closed helium refrigerator allowing one to perform measurements at low temperatures as well. Nowadays, the use of closed cycle refrigerator is particularly important because of the complexity and of the elevated costs in producing liquid helium. Furthermore, the world is already experiencing a shortage of helium.

In this work a Hall magnetometer built and coupled to a closed-cycle refrigerator is reported. The magnetometer was used to investigate in details the magnetic properties of the $(Fe_{0.6}Co_{0.4})_{0.35}(MnO)_{0.65}$ ferro-antiferromagnet composite from room temperature (*RT*) down to 10K and for applied magnetic fields up to 1 T. The effect of the cooling magnetic field H_R in the exchange-bias field (H_{EB}) was investigated for the first time in this sample material. The dependence of H_{EB} with H_R was qualitatively accounted for by a model proposed by Kagerer, Binek and Kleemann [4].

2. Details and operational principle

The magnetometer was built using two small size GaAs Toshiba Hall sensors (THS118). The sensor are 0.6 mm thick and they have a superficial area of 1.5×1.7 mm^2. The sensors were mounted side by side in a planar configuration 2 mm far apart from each other. They were assembled in a PPMS sample mounting support used for transport measurement [5]. An adapter was built to couple the PPMS support to a Displex system (Advanced Research Systems) allowing one to vary the temperature T in the range 10 – 300 K (see Fig. 1). The control electrical current of both Hall sensors were connected in series making use of a single electrical current source.

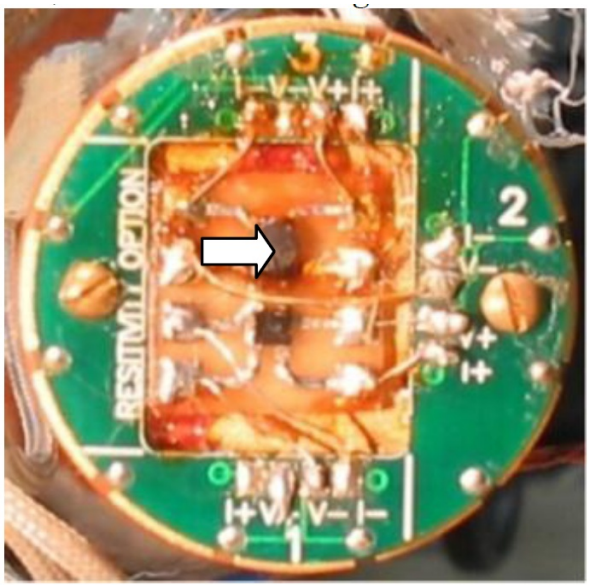

FIGURE 1. Hall magnetometer attached to the cold tip of a Displex system. The arrow points to a sample (disk) of $(Fe_{0.6}Co_{0.4})_{0.35}(MnO)_{0.65}$ fixed on the top of one of the Hall sensor.

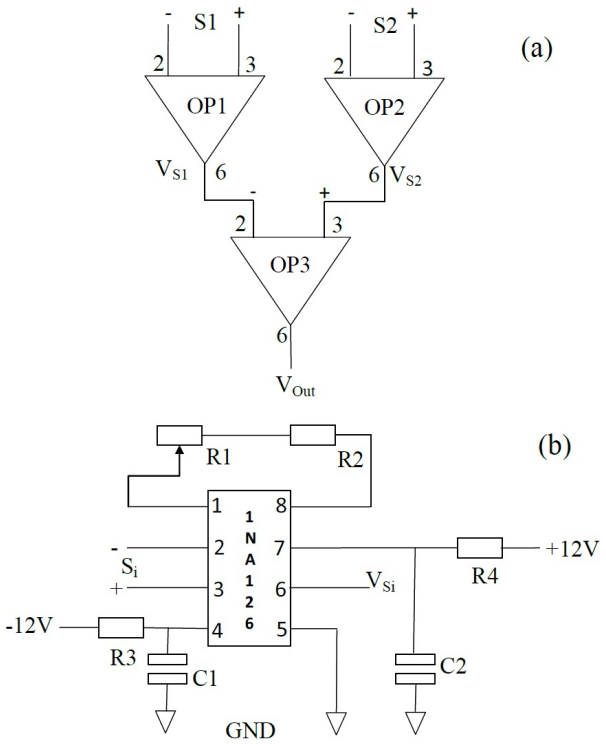

FIGURE 2. (a) Block diagram showing the electrical connections among the three operational amplifiers and (b) the connections and components for one of the operational amplification.

Misalignments in H with respect to the plane of the sensors plus small magnetic fields from the surround of the sensors are common source of undesirable signals (background). In order to reduce this background a two-stage differential amplifier circuit was built using three 1NA126 (Burr-Brown) operational amplifiers (Fig. 2a). The first stage (pre-amplifiers) provides independent amplification for the signal (Si) generated by each of the Hall sensors. The background subtraction is made at the second stage (amplifier) which works in a differential mode.

The connections and the components used to build the amplification circuits are shown in Fig. 2b. Batteries were used to feed the operational amplifiers with $\pm$ 12 V. Low-pass filters with cutting frequencies determined by $R3$, $R4$ (= 47Ω) and $C1$, $C2$ (100 nF) were used to reduce the noise from the batteries terminals. A 47 nF capacitor was added parallel to $C1$ e $C2$ for further reducing the high frequency noise. Each stage can provide a gain $G = 5 + R_0/(R1 + R2)$, where R_0 = 80 kΩ (op-amp internal impedance), $R1$= 100 kΩ (10 turns potentiometer) and $R2$ = 1 kΩ. G can be varied in the range 6-85 yielding an overall gain in the output signal from 36 to 7225. Individual gain for the pre-amplifiers helps one compensate small differences in the response of the Hall sensors reducing the background. The control electrical current can either be *dc* or *ac*. A Keithley voltmeter (model 180) and an EG&GPAR lock-in (model 5209) were used for dc and ac currents, respectively. The amplitude of the electrical current was varied from 0.1 to 3 mA and no significant self-heating was detected. A pair of Helmholtz may be used for measurements 3 mT while for H in the range $\pm$1 T we used a permanent magnet system made by Advancing Magnetic-Electronics. GPIB interface and the software LABVIEW were used for control and data acquisition.

The measuring principle is schematized in Fig. 3. First, the sample is fixed close to the active area of one of the Hall sensors. Next, the sample is magnetized by applying H in the plane of the Hall sensors and along the direction connecting them. The magnetized sample yields a dipolar field. The normal to the sensor component is proportional to the magnetization M yielding a Hall signal proportional to M as well. The differential mode helps one to eliminate small contributions (background) common to both sensors. The Hall magnetometer was calibrated measuring hysteresis loops of a small mass (6.1 mg) standard cylindrical sample of Ni with 0.5 mm of diameter and 1 mm of length. Figure 4 shows a typical hysteresis loop obtained at *RT*, H varying in the range $\pm$1 T, ac current with 1 mA of amplitude and frequency of 1 kHz, and G = 50. The value of the output voltage at the saturating magnetic field is taken to be equal to the total magnetic moment ($= 3.37 \times 10^{-4}$ A-m^2) of the Ni sample yielding

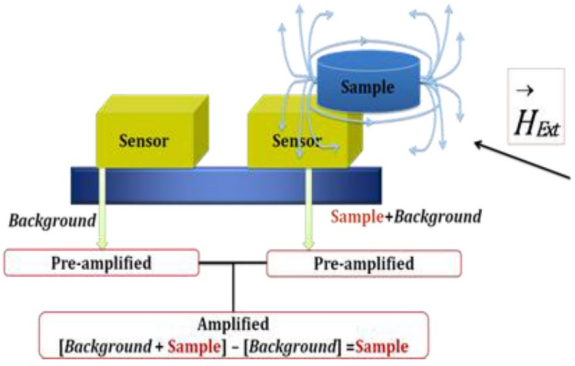

FIGURE 3. Block diagram showing the operational principle.

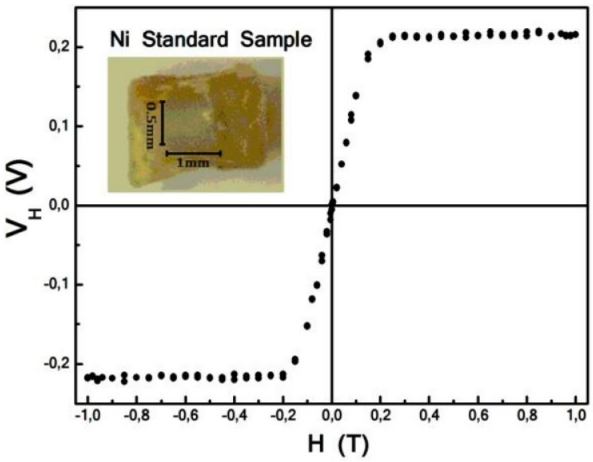

FIGURE 4. Room temperature hysteresis loop for the standard Ni sample. The inset is a photo of the Ni sample imbeded in epoxy.

a direct correspondence between the circuit voltage and the magnetic moment of the samples. The noise-to-signal ratio was estimated to be 1 part in 10^3.

3. Experimental results

The Hall magnetometer was used to investigated the magnetic properties of a 4.3 mg sample of the mechanically alloyed $(Fe_{0.6}Co_{0.4})_{0.35}(MnO)_{0.65}$ nano-composite from *RT* down to 10 K. A disk 0.3 mm thick and diameter of 2 mm was made by pressing (2 ton for 5 min) the powder sample. Scherrer analysis was performed in the X-rays diffractogram of the nanocomposite yielding 12.4 nm and 14.6 nm for the average particle size of the $Fe_{0.6}Co_{0.4}$ and of the MnO, respectively. MnO is antiferromagnet (AF) with a Néel temperature (T_N) of 117.7 K [6] while $Fe_{0.6}Co_{0.4}$ is ferromagnet with a Curie temperature (T_C) close to 800 K [7]. Above T_N the MnO particles behave as (paramagnetic) spacers for the ferromagnetic $Fe_{0.6}Co_{0.4}$ particles. However, below T_N the exchange coupling set the interaction among them on influencing the magnet parameters of the composite. Details of the sample preparation and some magnetic data above room temperature may be found elsewhere [8].

Two hysteresis loops measured using a VSM (vibrating sample magnetometer) and the Hall magnetometer are shown in Fig. 5. It was found that the two magnetization data are in good agreement within the resolution of the experiments.

Figure 6 shows hysteresis loops for the $(Fe_{0.6}Co_{0.4})_{0.35}(MnO)_{0.65}$ sample for two temperatures: 10 K and 300 K. It was found that the maximum value of $M(M(H$=1T)), the remanence (M_R) and the coercieve field (H_C) increases with decreasing T. The T-dependence of these parameters is shown in Fig. 7a and 7b. Below T_N an excess in the magnetization is observed in both $M(H$=1T) and M_R data. H_C was found to deviate from a $T^{3/4}$ behavior predicted by the Stoner-Wohlfarth model for randomly packed non-interacting single-domain particles [10].

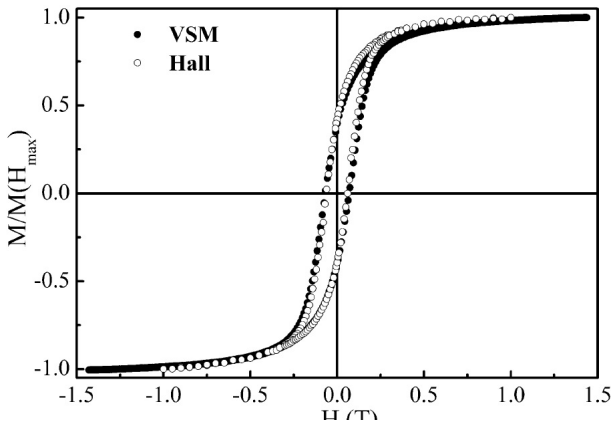

FIGURE 5. Hysteresis loops for $(Fe_{0.6}Co_{0.4})_{0.35}(MnO)_{0.65}$ measured at *RT* using a vibrating sample magnetometer (closed circles) and the Hall magnetometer (opened cycles).

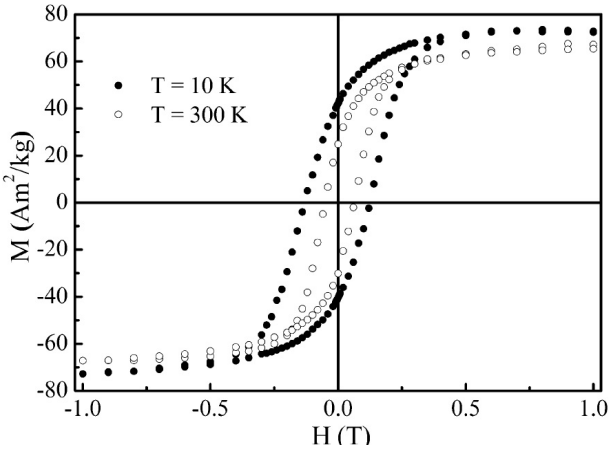

FIGURE 6. Hysteresis loops for $(Fe_{0.6}Co_{0.4})_{0.35}(MnO)_{0.65}$ measured at room temperature and for T = 10 K.

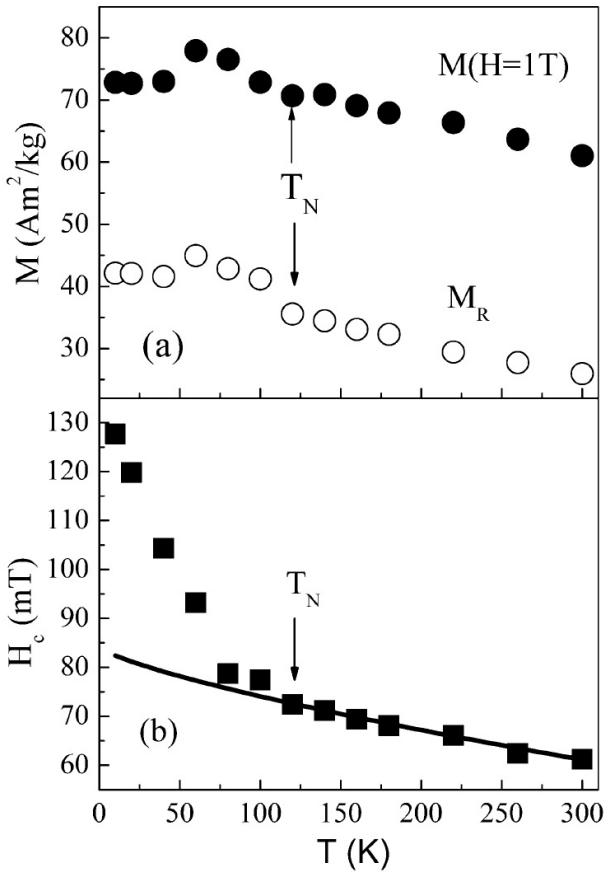

FIGURE 7. Temperature dependence of $M(H$=1T) and of the remanence (a), and of the coercive field (b). The solid line in (b) is a fit to the data using the Stoner-Wohlfarth model.

The T-dependence of the exchange-bias field has already been investigated and the results were taken by cooling the sample from 300 K to a given value of T (below T_N) and with H_R = 2 T [9]. However, the influence of H_R in the exchange-bias effect was not investigated in this sample material up to now. Thus, the magnitude of the exchange-bias field (H_{EB}) was measured using the Hall magnetometer and

by cooling the sample from 300 K to 10 K for different values of the cooling field ($0 \leqslant H_R \leqslant 1$ T). The dependence of H_{EB} with H_R is shown in Fig. 7 (symbols). H_{EB} was found to increase for increasing values of H_C, it reaches a maximum value (=22.5 mT) for H_R = 0.5 T and it diminishes when H_R is further increased, yielding 17 mT for H_R = 1 T. The solid line in Fig. 7 is a best fit to the data of a model proposed Kagerer, Binek and Kleemann [4]. In this model the exchange-bias field is mainly determined by the competition between the exchange energy at the FM-AF interface and the Zeeman of the AF spin with the cooling field. For low values of H_R the exchange term dominates while for high values of H_R is the Zeeman term which becomes more important. The roughness (α) does also play an important role in the model. The fitting yielded J/k_BT= 0.05074, $g\mu_B/k_BT$ = 6.77892 T^{-1},H_S = 0.4 T and α = 0.02956 where J is the exchange energy and H_S is the saturation magnetic field. g, μ_B and k_B are the g-factor, the Bohr magneton and the Boltzmann constant, respectively.

It is important to mention that other sample materials were investigated using the Hall magnetometer described in the present work. Among them are pieces of ribbons of soft-ferromagnetic amorphous materials. High magnetic permeability is characteristic of some of these materials. Thus, demagnetizing field may influence the magnitude of the magnetic susceptibility measured in pieces of ribbons made from ferromagnetic amorphous materials. Moreover, most of the techniques used for measuring magnetization require the use of small samples. Since the Hall magnetometer measure the magnetic dipole field emerging from one of the tips of the ribbon it does not present this constraint. Indeed, it showed to be quite useful in studying pieces of samples 10 cm long. The low-T data presented in here are also in good agreement with those reported in ref. 9 and that were obtained by using SQUID and extraction magnetometries. Finally, the use of the Hall magnetometer is not restricted to the range of temperatures and applied magnetic fields span in the present work. Indeed, the THS118 Hall sensors were found to be useful down to the miliKelvin regime and up to 20 T [11]. Since our magnetometer was assembled in a PPMS sample mounting support it can also easily be mounted in a PPMS as proposed by Candini and Afronte [5].

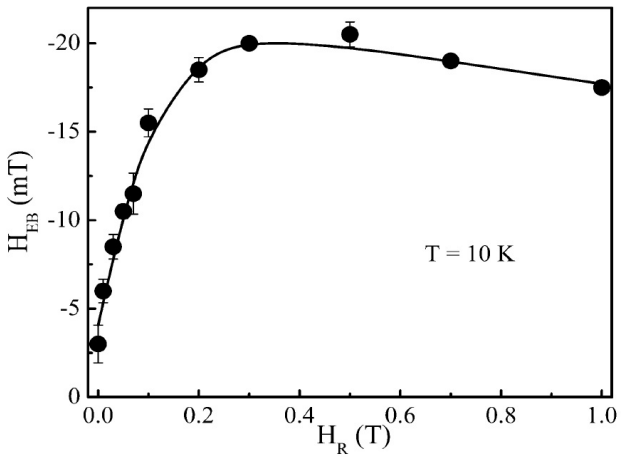

FIGURE 8. Dependence of the exchange-bias field with the cooling magnetic field for a sample of $(Fe_{0.6}Co_{0.4})_{0.35}(MnO)_{0.65}$. The solid line is a fit of a model discussed in the main text.

4. Conclusions

In summary, a differential Hall magnetometer was assembled in a Displex system. The magnetometer was found to be suitable for measuring hysteresis loops from room temperature down to 10 K. The Hall magnetometer was used to investigate the low temperature magnetic properties of the nanocomposite $(Fe_{0.6}Co_{0.4})_{0.35}(MnO)_{0.65}$. The effect of the cooling field H_R in the exchange-bias field H_{EB} of this sample material was studied for the first time. The dependence of H_{EB} with H_R was found to follows the general behavior predicted by a current theoretical model.

5. Acknowledgements

We thank W. G. Clark for providing the Hall sensors and L. R. S. Araújo and G. F. Barbosa for preparing some of the samples used for testing the magnetometer. Thanks are also due to S. R. P. da Silva (machine shop) and M. A. do Nascimento (electronics shop) for technical assistance. This work was partially supported by CNPq, FINEP, CAPES and FACEPE (Brazilian Agencies).

1. W. Viehmann, *Rev. Sci. Instrum.* **33** (1962) 537.
2. P.A. Besse, G. Boero, M. Demierre, V. Pott, and R. Popovic, *Phys. Letts.* **80** (2002) 4199.
3. Y. Li, P. Xiong, S. Molnar, S. Wirth, Y. Ohno, and H. Ohno, *App. Phys. Letts* **80** (2002) 4644.
4. B. Kagerer, Ch. Binek, and W. Kleemann, *J. Mag. Magn. Mater.* **217** (2000) 139.
5. A. Candini, and M. Afronte, *Quantum Design Application Note*, **1084-701** (2008) Rev. A0.
6. J.L. Shapiro, B.F. Woodfield, R. Stevens, J. Boerio-Goates, and M. Wilson, *J. Chem. Thermod.* **31** (1999) 725.
7. J.A. Oyedele, and M.F. Collins, *Phys. Rev. B* **16** (1977) 3208.
8. L.R.S. Araujo, F.C. Montenegro, and D.R. Cornejo, *J. Mag. Mag. Matls.* **320** (2008) e343.
9. L.R.S. Araujo, and F.L.A. Machado, *J. of Phys.: Conf. Series* **200** (2010) 072005.
10. J. Garcia-Otero, A.J. Garcia-Bastida, and J. Rivas, *J. Mag. Mag. Matls.* **189** (1988) 377.
11. E.C. Palm, and T.P. Marphy, *Rev. Sci. Instrum.* **70** (1999) 237.